CORROSION SCIENCE AND TECHNOLOGY, Vol.5, No.4(2006), pp.117~122

Hydrogen Diffusion in APX X65 Grade Linepipe Steels

†Gyu Tae Park, Seong Ung Koh, Kyoo Young Kim, and Hwan Gyo Jung[1]

Department of Materials Science and Engineering, Pohang University of Science and Technology, San 31, Hyoja-Dong, Nam-gu, Pohang 790-784 Korea
[1]Technical Research Center, POSCO Geodong-Dong, Pohang 790-704 Korea

Hydrogen permeation measurements have been carried out on API X65 grade linepipe steel. In order to study the effect of steel microstructure on hydrogen diffusion behavior in linepipe steel, the accelerated cooling condition was applied and then three different kinds of microstructures were obtained. Hydrogen permeation measurement has been performed in reference to modified ISO17081 (2004)[1)] and ZIS Z3113 method. Hydrogen trapping parameters in these steels were evaluated in terms of the effective diffusivity (D_{eff}), permeability ($J_{ss}L$) and the amount of diffusible hydrogen. In this study, microstructures which affect both hydrogen trapping and diffusion were degenerated pearlite (DP), acicular ferrite (AF), bainite and martensite/austenite constituents (MA). The low D_{eff} and $J_{ss}L$ mean that more hydrogen can be trapped reversibly or irreversibly and the corresponding steel microstructure is dominant hydrogen trapping site. The large amount of diffusible hydrogen means that corresponding steel microstructure is predominantly reversible. The results of this study suggest that the hydrogen trapping efficiency increases in the order of DP, bainite and AF, while AF is the most efficient reversible trap.

Keywords *: hydrogen diffusion, linepipe steel, hydrogen permeation measurement, hydrogen trapping*

1. Introduction

For transportation of oil and gas which contain hydrogen sulfide (H_2S), the application of linepipe steel is limited due to corrosion problems induced by hydrogen. Hydrogen induced cracking (HIC) and sulfide stress cracking (SSC) are the major problems of linepipe steels used in the sour environment.[2)-3)] When the linepipe steel is exposed in acid solution containing H_2S gas, hydrogen is produced by surface corrosion reaction of steel. In the presence of H_2S gas, recombination of hydrogen atoms into hydrogen molecules is retarded due to poisoning effect of H_2S. And then hydrogen atoms can easily diffuse into steel matrix and are trapped at defects susceptible to HIC.

Although the effect of microstructure on HIC and SSC of high strength linepipe steel has been exclusively investigated, the effect of microstructure on hydrogen diffusion behavior is unclear.[4)-5)] It is well known that acicular ferrite is the most desirable steel microstructure because it shows optimum mechanical properties and high SSC resistance.[4)] However, clear explanation about the role of acicular ferrite on hydrogen diffusion has not been reported. Therefore, it is worthwhile to study the effect of steel microstructure on hydrogen diffusion behavior in order to clearly understand the failure of linepipe steels induced by hydrogen.

†Corresponding author: pentium@postech.ac.kr

2. Experimental procedure

2.1 Preparation of test steel

Table 1 lists the chemical composition of tested steels. They are equivalent to API X65 grade. Various microstructures were obtained by controlling the start cooling temperature and finish cooling temperature.

All specimens were ground up to #2,000 with sand paper and then mechanically polished with 1um diamond suspension.

For microstructural observation, the specimens were degreased with acetone and etched with a nital solution (a mixture of 5% nitric acid and ethanol). The microstructure was examined with optical microscope (OM) and scanning electron microscope (SEM). After tint etching,

Table 1. Chemical composition of tested steels. (wt%)

C	Mn	Si	P	S	Al	Ca	Nb+ V+Ti	Cu+ Ni	Cr+ Mo
0.045	1.25	0.2	0.005	0.002	0.08	0.002	0.115	0.4	0.18

the area fraction of MA was determined by an image analysis. Second phases have been characterized in terms of their morphologies and hardness value. The hardness of single grain was measured using ultra-micro Vicker's hardness tester with denting load and dwelling time being 10 gf and 10 sec respectively.

2.2 Electrochemical hydrogen permeation measurement

Modified ISO17081 (2004) standard method was used in order to study the hydrogen diffusion behavior through the thin steel membranes.[8)-9)] Fig. 1 shows the schematics of electrochemical hydrogen permeation testing cell. Specimen has 30x30 mm^2 in area with thickness being about 1mm. The specimen was prepared from the region parallel to rolling direction at t/4 position where t was the thickness of steel plate. Both sides of the specimen were ground up to #2,000 with sand paper. The oxidation side of the specimen was electrochemically deposited with palladium (Pd) in order to ensure the hydrogen oxidation.[6)]

After cleaning the specimen with ethanol, specimen was located and sealed between two electrochemical cells. An area of 10.5x10.5 mm^2 was exposed to each electrolyte inside the cells. Although the ratio of radius to thickness is smaller than is recommended by the standard test method, preliminary experiment showed that the dimension of the specimen selected for this study was thick enough to ensure the volume controlled diffusion.[11)] The hydrogen charging compartment was filled with NACE TM0177-02A solution (a mixture of 5.0wt% NaCl and 0.5wt% glacial acetic acid dissolved in distilled water). Before pouring the test solution into the cell, it was deaerated with N_2 and saturated with H_2S (P=1atm). During the hydrogen permeation measurement, H_2S gas was continuously bubbled through this solution in order to keep the positive pressure of H_2S. The pH value of test solution just before experiment was about 2.95. The oxidation compartment was filled with 0.1 N NaOH solution. For deaeration, N_2 gas was continuously bubbled through this solution.

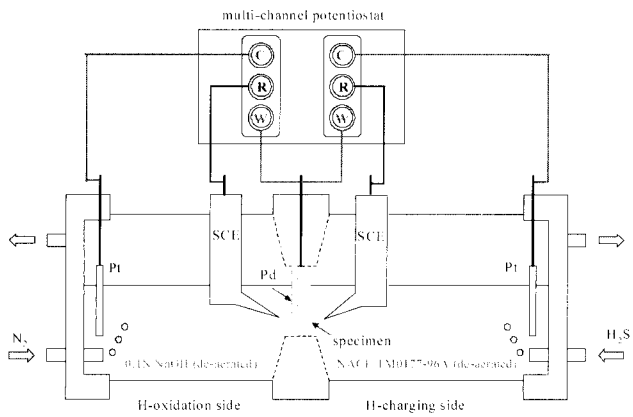

Fig. 1. Schematic of electrochemical hydrogen permeation cell

Potential applied at the hydrogen oxidation side was maintained 250 mV vs. saturated calomel electrode (SCE) at which dominant oxidation reaction was hydrogen oxidation. At this potential, atomic hydrogen atoms which diffuse through steel membrane are oxidized. Background current (anodic current without hydrogen oxidation) was below about 2 uA cm^{-2}. Once background current was stabilized, prepared NACE solution was poured into the hydrogen charging compartment. The electrochemical states of hydrogen charging compartment were freely corroding condition and galvanostatically polarized condition with cathodic current of 500 μA, respectively. And then oxidation current was measured for 1 hr of test duration. NaOH solution was continuously de-oxygenated by N_2 bubbling and NACE solution was continuously saturated with H_2S by H_2S bubbling. All measurements were performed at room temperature.

2.3 Data analysis

The hydrogen flux (mol H m^{-2} s^{-1}) through the steel specimen was measured in terms of steady-state current density, i_{ss}, and then it was converted into hydrogen flux according to the following equations.[7)-8)]

$$J_{ss} = \frac{i_{ss}}{nF} \tag{1}$$

The permeability (mol H m^{-1} s^{-1}) is defined as

$$J_{ss}L = \frac{i_{ss}L}{nF} \tag{2}$$

where n is the number of electrons transferred, F the Faraday's constant, L the specimen thickness, and J_{ss} the steady-state hydrogen flux. The effective diffusivity (D_{eff}) was determined by the time-lag method;

$$D_{eff} = \frac{L^2}{6t_{lag}} \tag{3}$$

where t_{lag} is the time at $J(t)/J_{ss}$ = 0.63.

2.4 Measurement of diffusible hydrogen content

Modified ZIS Z3113 method was used to measure diffusible hydrogen content. Fig. 2 shows the schematics of testing apparatus for ZIS Z3113 glycerin method. Standard HIC specimens immersed in NACE TM0177-02A solution for 96 hrs were used for this test. After 96 hrs of immersion in test solution, specimens were quickly

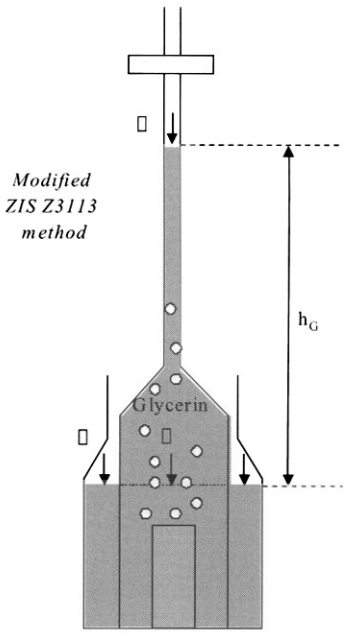

Fig. 2. Schematic of ZIS Z3113 glycerin method; ①+②=③, ①: pressure by evolved hydrogen, ②: pressure by glycerin with height h_G and ③: atmospheric pressure

cleaned with cold water (0℃) to prevent the release of diffusible hydrogen out to air. And then they were placed in 45 ℃ liquid glycerin, which could sufficiently release the diffusible hydrogen from the specimen. After sufficient release of diffusible hydrogen, the volume of collected hydrogen gas was measured and the amount of diffusible hydrogen was determined.

3. Results and disccution

3.1 Microstructure

Fig. 3 shows the typical steel microstructures at t/4 position. The primary phases are qusi-polygonal ferrite (QPF) or mixture of QPF and acicular ferrite (AF). The dark grains in the figs. are considered as the secondary phases and their characteristics were characterized in terms of morphology and micro-hardness. Fig. 4 shows SEM images of the typical second phases. They are DP, bainite and MA constituents and their size is below about 5 um.

In general, DP is called as pseudo-pearlite without lamellar structure. It is transformed from austenite when the cooling rate is higher than that for the formation of pearlite and lower than that for the formation of bainite. The micro-hardness of DP is about Hv230.

Observed bainite is coarse and elongated along the rolling direction. Bainite has many carbide particles and MA constituents in a grain. Micro-hardness of bainite is over about Hv280. It is assumed that such high micro-hardness is due to the high density of carbide particles and the existence of MA constituents.

Inclusions are globular-shaped and contain Al-Ca-Si-O. The average size of them is about 1.5 ㎛ in diameter. Spheroidization of inclusions was enhanced due to Ca-

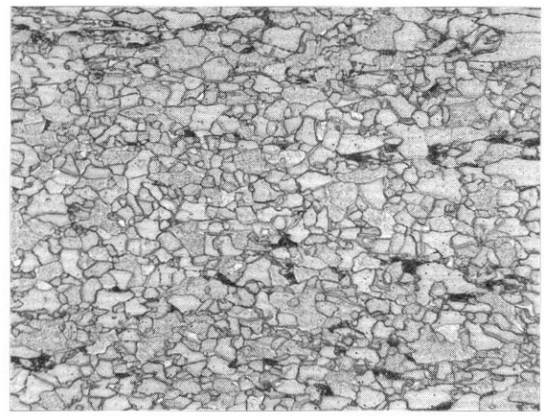

(a) QPF + DP

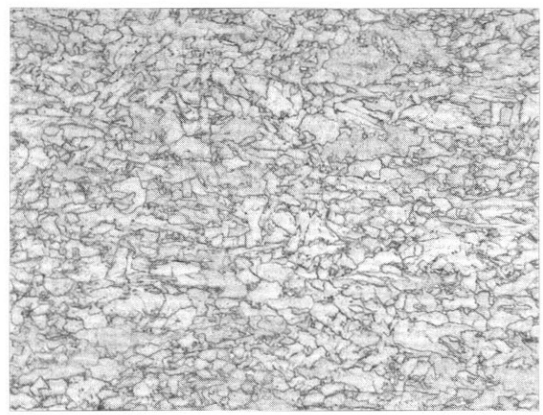

(b) QPF + AF

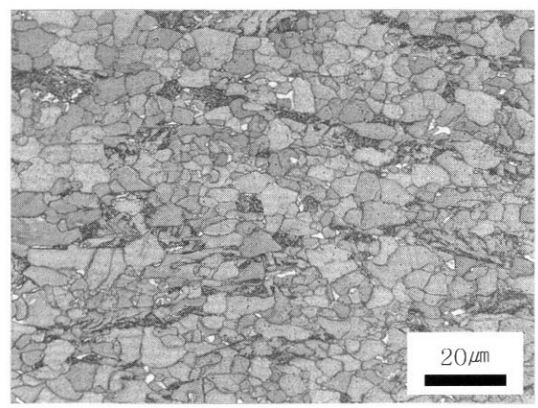

(c) QPF + bainite

Fig. 3. Typical microstructure of test steels; (a) S3, (b) and (c) S9

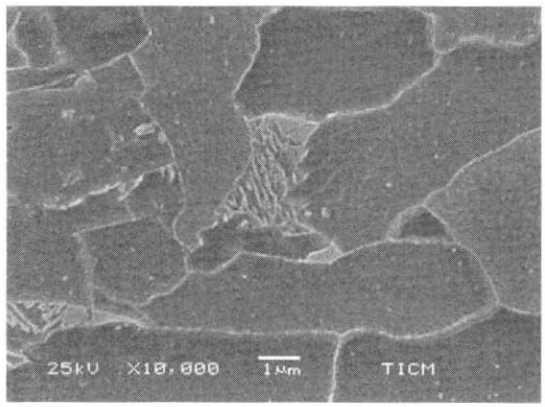

(a) DP

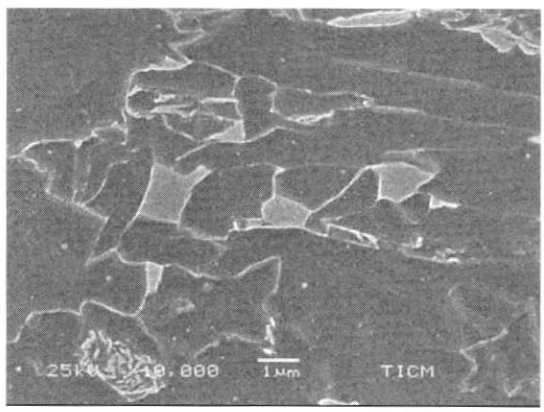

(b) MA constituents

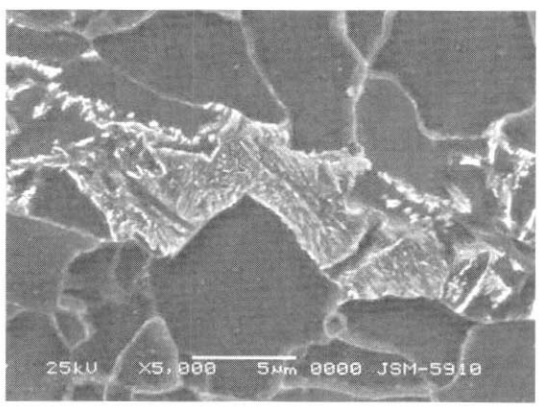

(c) bainite

Fig. 4. SEM photographs of second phases; (a) S1, (b) S2 and (c) S9

treatment during steelmaking process. Manganese sulfide (MnS) inclusions with elongated band-pattern were not observed. Size, distribution and composition of inclusions are similar for all specimens because the identical steelmaking process was applied for all steels. Therefore, the irreversible trapping effect at inclusion interfaces is considered to be the same for all specimens and the role of inclusions on hydrogen diffusion behavior is excluded.

3.2 Hydrogen permeation

Hydrogen charging surface of the specimen was galvanostatically polarized to cathodic current of 500 μA. The potential measured in this state was constantly maintained about -690 mV vs. SCE. The pH of NACE solution was nearly constant during the test duration. Pourbaix diagram represents that the steel does not corrode in this environmental condition and it also means that surface condition does not change during the test duration.

Fig. 5 shows the hydrogen permeation curves for the Steels S4, S5 and S6. Oxidation current increases with time, and the steady state current is eventually obtained after about 1 hr.

The D_{eff} and $J_{ss}L$ are listed in Table 2. Steel S6 having large area fraction of AF and MA constituents shows the lowest $J_{ss}L$ and D_{eff}. The $J_{ss}L$ and D_{eff} decrease with increase in the total area fraction of AF and MA constituents. In general, AF in high strength low alloy (HSLA) steels is defined as highly substructured non-equiaxed phase and their transformation kinetics contain both the diffusion and shear transformation. It contains high dislocation density in the form of dislocation tangles. Dislocation is well known as the hydrogen trapping site and increases the amount of diffusible hydrogen by acting as reversible hydrogen sink. It has been reported that highly tangled dislocation density in AF leads to deflection of hydrogen transport, so that delays the hydrogen diffusion.[1)]

To compare the microstructural effect of DP and bainite on hydrogen diffusion, Steels S7 and S9 were compared. Steel S9 having fine ferrite and bainite shows lower D_{eff} and $J_{ss}L$ compared to Steel S7 having coarse ferrite and

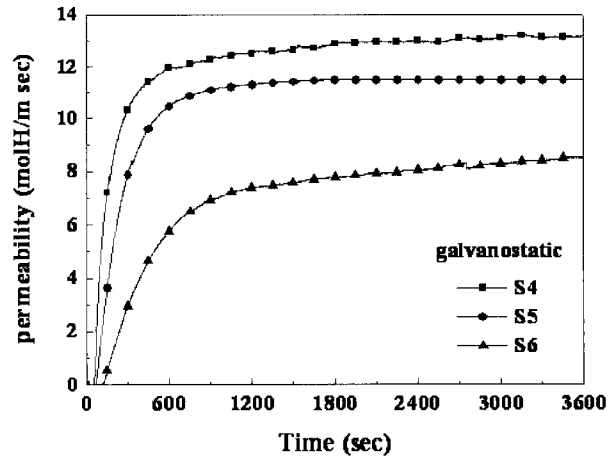

Fig. 5. Hydrogen permeability at hydrogen oxidation compartment

Table 2. Hydrogen permeation measurement results

	Micro-structure	Fraction of DP/AF/BF	M/A fraction	C_{eff} ($x10^{-10}$ m^2sec^{-1})	$J_{ss}L$ ($x10^{-9}$ molH $m^{-1}sec^{-1}$)
S1	F/DP	4.73	0.94	-	-
S2	F/AF	10.94	1.4	5.47	13.9
S3	F/AF	22.79	3.64	4.08	12
S4	F/DP	3.75	1.28	9.21	13.3
S5	F/AF	8.1	2.86	7.39	11.5
S6	F/AF	8.12	5.73	3.11	8.47
S7	F/DP	3.93	0.88	7.54	12.9
S8	F/BF	29.98	1.21	2.21	11.8
S9	F/BF	9.38	4.45	4.41	12

DP. This means that bainite delays the hydrogen diffusion more effectively than DP. Several studies have suggested that the pearlite blocks located at the ferrite layers may possibly retard the permeation of hydrogen in the ferrite/pearlite structure, the dominant transportation path of hydrogen being through the ferrite layer as well as along the ferrite grain boundaries and ferrite/pearlite interfaces.[10] Luu has reported that the bainitic ferrite consists of inter-lath cementites whose interfaces between steel matrix act as obstacles for hydrogen diffusion.[3]

The D_{eff} and $J_{ss}L$ decrease with increase in the amount of MA constituents. This means that MA constituents, which consist of martensite and retained austenite (RA), act as hydrogen trapping sites. Chan has reported that RA itself does not significantly trap hydrogen, but the interfaces between RA and martensitic plates may be the possible trapping sites.[11]

Steel S2 having ferrite and AF shows lower D_{eff} and $J_{ss}L$ than Steel S8 having ferrite and bainite. This means that hydrogen trapping efficiency is higher for AF than for bainite.

3.3 Diffusible hydrogen

Another method to evaluate hydrogen diffusion in steels is ZIS Z3113, so called glycerin method. Diffusible hydrogen content is easy to measure with this method and the results are very reproducible. Fig. 6 shows the amount of diffusible hydrogen in specimens having different microstructures. As shown in this graph, steels having AF show large amount of diffusible hydrogen while steels having ferrite and DP show lower amount than steels having AF. The amount of diffusible hydrogen increases in the order of DP, bainite and AF. Diffusible hydrogen is characterized as freely diffusing hydrogen through steel lattice along with hydrogen reversibly trapped at such

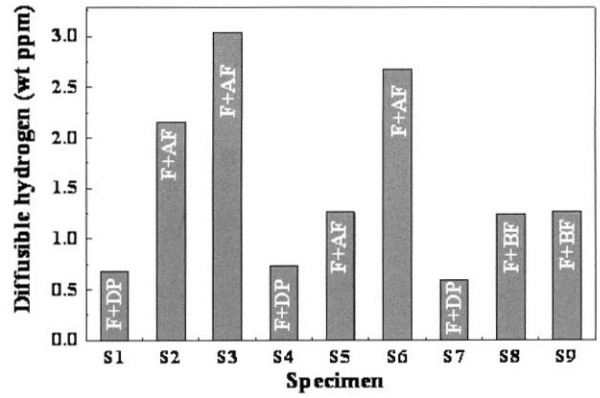

Fig. 6. ZIS Z3113 Glycerin method results

defects as dislocations and grain boundaries. In this experiment, results show that AF is reversible trap and trapping efficiency is very high.

4. Conclusions

The effect of steel microstructure on hydrogen diffusion in linepipe steel was studied using electrochemical method and glycerin method. The results are summarized as follows:

1) All the microstructural components, *ie* degenerated pearlite, acicular ferrite, bainite and martensite/austenite constituents, affect both the hydrogen trapping and diffusion.

2) The ability of microstructure to uptake hydrogen is explained in terms of the D_{eff} and $J_{ss}L$. The low values of D_{eff} and $J_{ss}L$ mean that more hydrogen can be trapped in steel and the corresponding steel microstructure is dominant hydrogen trapping site. The results of this study suggest that the hydrogen trapping efficiency increases in the order of degenerated pearlite, bainite and acicular ferrite, with acicular ferrite being the most efficient.

3) The amount of diffusible hydrogen is largest in the steel having acicular ferrite and increases with increase in the area fraction of acicular ferrite. This means that acicular ferrite reversibly traps hydrogen atoms and trapping efficiency is higher than any other microstructural component among all tested microstructures.

References

1. ISO 17081:2004(E), ISO, (2004).
2. NACE Standard MR0175-2002, NACE, Houston (2002).
3. W. C. Luu and J. K. Wu, *Corros. Sci.* **38**, 239 (1996).
4. Y. Inohara, N. Ishikawa, and S. Endo, *Proc. of 13th Int. Offshore and Polar Eng. Conf.*, p.60 (2003).
5. S. U. Koh, J. S. Kim, B. Y. Yang, and K. Y. Kim,

Corrosion, **60**, 244 (2004).
6. P. Manolatos, M. Jerome, and J. Galland, *Electrochim Acta*, **40**, 867 (1995).
7. J. Crank, The Mathematics of Diffusion, p.44. Oxford University Press (1979).
8. N. Boes and H. Zuchner, *J. the Less-Common Metals*, **49**, 223 (1976).
9. M. A. V. Davanahan and Z. Stachruski, *J. Electrochem. Soc.*, **111**, 619 (1964).
10. L. Tau and S. L. I. Chan, *Mat'l Letters*, **29**, 143 (1996).
11. S. L. I. Chan, H. L. Lee, and J. R. Yang, *Mat'l Trans.* **22A**, 2579 (1991).
12. B. Y. Yang, Y, H, Jung, and K. Y. Kim, "The study of hydrogen permeability of API-X60, X65 and improvement of the test method for SSCC", POSCO Research Report, p.157 (2002).